

Flash Sintering of Alumina: Effect of Different Operating Conditions on the Densification

Behaviour

Mattia Biesuz^{1*} and Vincenzo M. Sglavo^{1,2}

¹ Department of Industrial Engineering, University of Trento

Via Sommarive 9, 38050 Trento (ITALY)

² INSTM Research Unit

Via G. Giusti 9, 50121 Firenze (ITALY)

Abstract

Pure α -alumina samples produced by uniaxial pressing were flash sintered under electrical fields ranging from 500 V/cm to 1500 V/cm in constant heating rate experiments. Sintering temperature significantly decreased with the applied E-field even down to $\approx 900^\circ\text{C}$ at 1500 V/cm. The onset temperature for flash sintering can be successfully modelled as a function of the applied voltage. The sintering temperature is shown to be also strongly affected by the electrodes material used during the treatment: by using silver or carbon electrodes the sintering temperature is about 300°C lower than in the case where platinum electrodes are used. In addition bulk density and porosity of the sintered alumina ceramic are strongly correlated to the imposed current limit. Power dissipation was analysed before and during flash sintering; the activation energy for conduction was calculated in both the cases, indicating that the process is based on ionic diffusion phenomena. Finally, it was shown that during Flash Sintering the activation energy for conduction decreases, this suggesting the occurrence of physical or structural modifications induced by the current localization at the grain boundaries.

* Corresponding author, email: mattia.biesuz@unitn.it

Keywords: Flash Sintering, Alumina, Joule Heating, Conduction, Activation Energy

1 Introduction

The reduction of environmental, energetic and economic costs is one of the main concerns for the ceramic industry of the present century. Several recent studies [1-14] have shown that the application of an electrical field is very effective in reducing sintering time and temperature, thus allowing more limited energy consumption and CO₂ emissions. In particular, at specific electrical field and temperature the so called Flash Sintering (FS) can be observed [1-14]. This phenomenon, which is accompanied by an abrupt increase in the material conductivity, allows to reduce the sintering time to few seconds and typically allows the densification of ceramics at temperature much lower than the conventional one. Such sintering technique has been studied on many semi-conductive (YSZ [1-5], GDC [6], SiC [7], ZrO₂-Al₂O₃ composites [8-9]), and electrically conductive (MnCo₂O₄[10-11], LSCF [12-13]) ceramics.

Although different theories have been developed for explaining such unusual behaviour, the mechanisms leading to material densification are still unknown. Some proposed theories involve the local heating at the grain boundaries [1,14] or the formation of Frenkel pairs [14,15] driven by the applied electrical field. Also Joule heating was suggested to be responsible for the rapid densification; nevertheless, some experimental results have shown that the sample surface temperature is far lower than that needed for conventional sintering in few seconds [3,15]. Recently, Todd et al. developed a model indicating that FS event is just induced by a thermal runaway of Joule heating [4]. They also demonstrated that the temperature in the sample core upon FS is much higher than that measured on the surface, although they also stated that *“the mechanistic details of densification remain uncertain”*. Thereby, the problem is still open and controversial.

Although FS has been demonstrated on several semi-conductive and conductive ceramics, very few works have been carried out on resistive materials. Cologna et al. performed some experiments on high purity alumina and concluded that this could not be flash sintered. It was also shown that alumina completely changes its electrical behaviour by doping with 0.25 wt% MgO and MgO-doped alumina was successfully flash sintered down to 1260°C [14].

In the present work, 99.8% pure alumina was subjected to flash-sintering experiments with the aim to understand the possible conduction mechanisms and the densification behaviour in a widely used resistive oxide ceramic. The study was carried out also to point out the influence of some operating conditions upon FS, such as electrical field intensity, current density and different electrodes material.

2 Experimental Procedure

Pure α -Alumina (Almatis, CT 3000 SG, $d_{50} = 0.6 \mu\text{m}$, $d_{90} = 3.0 \mu\text{m}$) with nominal composition Al_2O_3 99.8wt% - MgO 0.04wt% - Na_2O 0.03wt% - Fe_2O_3 0.015wt% - SiO_2 0.015wt% - CaO 0.015wt% was used in the present work. After the addition of 6 wt% distilled water, dog bone samples were produced by uniaxial pressing at 120 MPa. The thinner cross section of the pressed sample was 3 mm x 3.3 - 4 mm. Sintering tests were carried out in a Linseis L75 dilatometer with a constant heating rate of 20°C/min. A DC field was applied thorough a power supply (Glassman EW series 5 kV-120 mA) when the sample reached 350°C and it was maintained to a constant value until the current limit was reached. The field and the current density ranged from 250 to 1500 V/cm and from 2 to 7 mA/mm², respectively. The current intensity and the voltage were measured with frequencies of 1 Hz by a multimeter

(Keithley 2100). Once the current limit was reached, the current was let to flow for 2 min and then the system was shut down.

The samples were connected to the power supply by two platinum wires which were forced into the holes present on the opposite edges of the dog bone sample. For improving the electrical contact between the electrodes (platinum wires) and the ceramic different conductive paste were employed. The first one, used for the most of experiments, was a platinum-based paste (Sigma Aldrich). In addition, silver paste (Agar Scientific) and carbon cement (Plano GMBH) were used for comparison.

The density of the sintered samples was measured by the Archimede's method using a balance (Gibertini) with sensitivity of ± 0.1 mg. Only the constant-cross section part of the specimen between the two electrodes was used for the density measurements.

3 Results and Discussion

3.1 Effect of current, voltage and electrodes material

Figure 1 shows the effect of the electrical field on the sintering behaviour of alumina for samples treated with platinum electrodes. First of all, one can immediately point out that the considered material can be flash sintered under an electric field (E-Field) in excess to 500 V/cm; if a voltage of 250 V/cm is applied, the shrinkage is limited.

Sintering temperature significantly decreases at higher E-fields, up to 1500 V/cm, when the material sinters at around 920°C. Such evidences show a clear anticipated sintering process if compared to the results collected by Colonga et al. on 0.25 wt% MgO-doped alumina [14]: the onset temperature for flash sintering (FS), in fact, decreases of 120 – 230°C (under the same field). This anticipated sintering process can not be related to the different grain size [5], the powder used in the present work being coarser than that used by Colonga (100 –

300 nm). In addition, one can observe that the MgO-doped alumina used by Cologna et al. contains larger amount of impurities (0.25 wt%) if compared with the material used here. This suggests that the anticipated FS phenomena can be accounted for by some beneficial effect on corundum conductivity associated to the presence of different chemicals. As a matter of fact, elements with oxidation number lower than 3 (e.g, Mg^{++} or Ca^{++}) act as electrons acceptor [16,17] and promote the formation of oxygen vacancies [17-19], while elements with oxidation number higher than 3 (e.g., Si^{4+}) behave as donors [16,17] and should promote the formation of aluminium vacancies, as previously reported [19]. In this way both ionic and electronic conductivity increase as a result of larger vacancies concentration and narrower band gap for electrons jump in the conduction band, respectively.

Samples tested under low voltage (500-750 V/cm) exhibit two different densification mechanisms. The first occurs before the current limit is reached and is responsible for 3-6% linear shrinkage. The dilatometric plots are here characterized by a downward concavity.

The densification in this case is partially due to “conventional / thermal” sintering mechanisms. Nevertheless, one can observe that the shrinkage increases with the applied E-Field: therefore, an electrical contribution to densification is also clearly present. For this reason, such sintering mechanism can be defined just as Field Assisted Sintering (FAS).

The second part of the sintering process is characterized by an upward concavity in the dilatometric plots and it occurs just after the current limit is reached. This is the properly called Flash Sintering.

The samples tested under high voltage (1000-1500 V/cm) sinter at temperature lower than 1050°C and therefore FS is responsible for almost all the densification. In this case, the linear shrinkage upon sintering appears almost independent from the applied voltage.

On the basis of Fig. 1, one can point out that the final shrinkage and the sintering rate (the slope of the dilatometric plot) increase with the nominal current density. Also some physical properties of the sintered bodies, like apparent porosity and bulk density (Figure 2), are improved if a more intense current is applied. In fact, it is possible to achieve a huge decrease in the amount of open porosity by increasing the current from 2 to 4-5 mA/mm². For higher current a plateau is reached and no significant advantages can be achieved. Therefore, the nominal current density is always the key parameter controlling the sintering rate and the final density of the ceramic bodies. This is probably due to the higher specific power dissipation that are obtained increasing the current limit (as it will be shown in the following session).

Figure 2 shows two different trends. The first regards the sample sintered under low voltage (500 V/cm and partially 750 V/cm). As explained before, the densification phenomena in such samples have already been partially activated when the current limit is reached. It is possible to observe that the material is nearly fully dense with only 4 mA/mm² nominal current density and also the specimens sintered with 2 mA/mm² are characterized by a limited open porosity (~7%). Conversely, the specimens tested under E-Field in excess of 1000 V/cm are characterized by high apparent porosity (>20%) and limited density (< 3.1 g/cm³) when sintered with 2 mA/mm². These specimens reach a complete densification only with 5-6 mA/mm².

Figure 3 shows the specific power dissipation as a function of the furnace temperature. Two different regions can be identified: the first, with power dissipation lower than 25 mW/mm², is characterized by FAS; in the second one, there is instead an abrupt increase in power dissipation and FS occurs. This deviation from the normal linear-like behaviour, which is accompanied by a drop in the material resistivity, was observed by many authors [1,2,6,10]

usually in the power range 1-15 mW/mm³. Different reasons were proposed for explaining such a behaviour and among them the most discussed ones are local grain boundary heating [1,14], Frenkel pairs formation [14,15] and Joule heating (although some experimental results pointed out that this is not the fundamental densification mechanism [3,15]).

Even in the FAS region, the behaviour of the system is not perfectly linear, i.e. the slope of the curve is slightly increasing with 1/T. The reason behind such behaviour can be the presence of different conduction mechanisms, that with the higher activation energy being activated only at higher temperature [20-23]. Moreover, it should not be forgotten that the specimen undergoes to several modifications upon heating (i.e. necks formation provides a continuous and interconnected path for current flow) which can lead to an increase in conductivity.

In any case, a linear-like behaviour provides a quite good approximation of the power dissipation plot in the region before FS. The activation energy for the conduction mechanism was therefore calculated by interpolating the experimental data in a 250°C wide temperature range, before the deviation from linearity due to FS (as it is shown for example in Fig. 3 for a sample treated under 1500 V/cm); the calculation was carried out considering the plots recorded by using different electrodes material. The activation energy was estimated in 1.2±0.2, 1.2±0.1, 1.0±0.2 eV for platinum, carbon and silver electrode, respectively. Similar results were found by Cologna (1.5-2.3 eV) [14], Pan (1.5-2.4 eV) [20], Mohapatra (2-2.1 eV) [24] and Öijerholm (1eV) [25] who worked with dense alumina bodies. The calculated activation energies are far lower than the band gap for pure corundum (8.7-10.8 eV) [26-29]. The presence of the grain boundary (more “disordered” material) can only partially account for a narrower band gap: for example, values around

3.2-8.7 eV are reported for amorphous alumina [28,29,31], still far larger than those estimated here.

The presence of aliovalent atoms can also change the difference between conduction and valence band; for example, magnesium can act as electron acceptor or silicon as electron donor [16,17]. Several works are reported in the literature showing the band gap evolution as a function of different doping elements; nevertheless, band gap energies around 4-5 eV are reported [29,30], still larger than the results previously reported.

Although a partial electronic contribution to conduction can not be completely excluded, it does not seem to be the main conduction mechanism. Some clear findings can support such hypothesis. In fact, it is reported that electronic conduction in alumina is activated at high temperature, becoming predominant around 1400°C [20,32-35]. Other authors suggest that conduction is still ionic, and based on Al³⁺ diffusion, even at high temperature (1000-1650°C) [26].

The problem of diffusion in corundum is very controversial and very large data scatter is found for oxygen and aluminium self-diffusion. The most complete work summarizing the actual knowledge about this topic was produced by Heuer [36]. He reported many experimental data showing that, in most cases, the measured activation energy for lattice self-diffusion in alumina falls in the range 3-8 eV. It is to say that these measurements were often carried out using radiotracer at high temperature (>1300°C). In addition, it was shown that the grain boundary presence does not reduce these values enough for making them comparable with the conduction activation energy determined in the present study [36-38]. On the other hand, other experiments were carried out at lower temperature (usually <1200°C) by electrical test (i.e. EIS, interfacial polarization) fixing the energy barrier for Al and O self-diffusion in the range 0.8-2.4 eV [20,25,34,39]. Such values are in agreement with

those found in the present study and perfectly match with those (0.7 and 2.5 eV) obtained by several theoretical calculations [17,18,40,41].

Some explanation can be proposed for taking in account the observed differences:

- i. At high temperature the diffusion paths with higher energy barrier are activated [20-23]. It was shown that a transition between intrinsic and extrinsic diffusion can be observed around 1600-1650°C [21,22]. At lower temperature diffusion is “*impurity-controlled*” or “*structure-sensitive*” [21] or it is concentrated through fast paths like dislocation. Oishi et al. showed that in crushed alumina the activation energy for oxygen diffusion is reduced down to 1.87 eV as a result of the high concentration of line defects [42].
- ii. Some surface effect on diffusion can not be *a priori* excluded. Öijerholm and Pan pointed out that the activation energy for oxygen surface diffusion in corundum should be around 1 eV although even in this case a large scatter is reported [43,44].
- iii. Finally, one should consider that the presence of different point defects with net charge leads to the formation of clusters by electrostatic interaction. This phenomenon is well-known in doped alumina [17-19,41]. In particular, clusters binding Mg'_{Al} and V_{O}'' were extensively studied and binding energies in the range 1.3-3.5 eV were calculated. Therefore, as it was suggested by Tewari [18], when the activation energy for diffusion is measured, the contribution of clusters can not be neglected. Tewari estimated that the Mg^{++} presence leads to an increased energy barrier for V_{O}'' diffusion of 2-3 eV, this accounting for the difference between calculated and measured activation energy by radiotracer. It is to say also that the activation energy measured by electrical method [20,25,34,39] are in good

agreement with the theoretical values [17,18,40,41] and with those found in the present work. This can be accounted for by the fact that clusters are broken by the E-Field application and, once broken, the rapid vacancies movement can inhibit their reformation.

Figure 4 shows the sintering temperature as a function of the E-Field when different electrode materials are used. It is possible to observe that by changing the electrode also the system alters its response upon sintering. In particular, by adding silver paste, the onset sintering temperature is reduced of about 250°C with respect to the use of platinum electrodes. The carbon cement determines a behaviour more similar to Pt paste although the samples are sintered at lower temperature. The improvement of electrode contacts, accompanied by a resistance decrease, does not seem to be a reasonable justification for such large difference. It seems that carbon and especially silver are somehow catalytic for some reactions at alumina/metal electrode interface, increasing the conductivity of the system. Conversely, platinum, being a noble metal, does not produce any interaction. One can speculate that a variation in the oxidation state of carbon promotes the formation of defect in Al_2O_3 ; i.e., crystal defects like oxygen vacancies, can be produced in alumina by a combined effect of anodic polarization and carbon oxidation leading to increased conductivity.

The presence of silver can also enhance the conductivity in two ways.

- i. It is extensively reported that Ag^+ diffusion coefficient in corundum is much higher than the self-diffusion coefficients for aluminium and oxygen [45,46]. Therefore, a conduction mechanism where silver ions are the main charge carriers can be suggested. Nevertheless, no evidence of silver presence were detected by EDS in the

central part of the dog bone sample used here. Moreover, the differences in the activation energies for Ag/C and Pt electrodes are not high enough for stating that different conduction mechanisms are activated.

- ii. Silver, being a monovalent ion, when substituting an aluminium ion can promote the formation of crystal defects (as it was reported for other aliovalent species [16-19]).

The result is an increased defect population, with enhanced conductivity.

The experimental data, relating the E-Field and the onset temperature for FS, were fitted by recursive method using the model developed by Todd et al. [4] for isothermal FS experiments. The model is based on a power balance between the electrical power and the heat dissipated by radiation. The equations relating the onset furnace temperature for FS and the applied electrical field are:

$$\frac{E^2 V}{\rho_0} \exp\left(\frac{-Q}{R(T_f + \Delta T)}\right) = S \sigma \varepsilon \left((T_f + \Delta T)^4 - T_f^4 \right) \quad (1)$$

$$\frac{E^2 V}{\rho_0} \frac{Q}{R(T_f + \Delta T)^2} \exp\left(\frac{-Q}{R(T_f + \Delta T)}\right) = 4 S \sigma \varepsilon (T_f + \Delta T)^3 \quad (2)$$

where E is the E-Field, Q and ρ_0 the activation energy and the pre exponential constant of the resistivity respectively, T_f the furnace temperature, ΔT the sample overheat needed for FS, σ the Stefan-Boltzmann constant, ε the emissivity, R the universal gas constant, V and S the volume and the surface of the sample, respectively. Eq. 2 can be also written as:

$$E^2 = \frac{4 S \sigma \varepsilon R \rho_0}{V} \frac{(T_f + \Delta T)^5}{Q} \exp\left(\frac{Q}{R(T_f + \Delta T)}\right) = A \frac{(T_f + \Delta T)^5}{Q} \exp\left(\frac{Q}{R(T_f + \Delta T)}\right) \quad (3)$$

where A is a constant. By combining Eqs 1 and 2 a relationship between the sample temperature needed for FS and the furnace temperature can be obtained:

$$\frac{4R}{Q} T_s^5 - T_s^4 + T_f^4 = 0 \quad (4)$$

where $T_s = T_f + \Delta T$. The application of this model to the given constant-heating rate FS is an approximation. In fact, it is assumed that the time needed for sample heating is always zero and this is not true since the sample has its own heat capacity. This is responsible for a delay in the FS events with respect to the model. Moreover, the sample temperature can not be homogenous (the surface is always colder because of the radiative heat exchange). Nevertheless, it is possible to hypothesize (also because of the very limited sample sizes) that this retardation is not much significant and, in any case, similar delay is present in all samples.

The experimental data were interpolated by a recursive method, as follows:

- i. The activation energy (Q) is assumed equal to 50 kJ/mol;
- ii. Using Eq. 4 and the experimental results for the onset furnace temperature (T_f), T_s was calculated for each sample by NSolve command in Mathematica®;
- iii. A new value for Q and for the constant A was estimated by Eq 3 using FindFit function in Mathematica®;
- iv. With the new Q value all the operations were repeated until Q changes less than 0.05 kJ/mol between two successive interactions.

The best fit was found using activation energies of 1.57, 1.37 and 1.32 eV for platinum, carbon and silver electrodes, respectively. These values are similar to those previously calculated from the slope of the power dissipation plots. As it is shown in Figure 4, the model provides a good approximation of the experimental results in the case of Pt and C electrodes, and the error is nearly negligible (always lower than 17°C) if Ag electrodes are used. The experimental data, which appear not perfectly fitted by the model, are those taken at 500 V/cm, especially for Pt and C electrodes; in this case, the samples are flash

sintered at temperature lower than that expected by the model. This is probably due to the fact that the material properties are changing upon heating, the specimens treated under limited voltage being already partially sintered when FS occurs. In this way a continuous path for current flow is formed, leading to a decrease in resistivity and anticipating FS. The data fitting obtained excluding the data at 500 V/cm gives activation energies of 1.53 and 1.34 eV for Pt and C electrodes, respectively, not very different from those previously calculated.

In any case, one can undoubtedly point out that the model provides a satisfactory fitting of the experimental data also for constant-heating rate FS experiments. The results are consistent and supported by the activation energy calculations previously carried out.

The electrodes material has also an important effect on the alumina densification. The total shrinkage upon sintering and the shrinkage after the current limit is reached and FS occurs are reported in Figure 5. One can observe that the material tested using Pt and C electrodes behaves more or less in the same way, while the samples sintered using Ag paste show much lower shrinkage. This result is supported also by the density and porosity measurements (Fig. 6), which clearly indicate that the specimens treated using silver electrodes are less dense and more porous. When Pt and C electrodes are used, the only difference (as shown in Figure 6) regards the samples treated under limited voltage (500-750 V/cm). In such case FAS - thermal sintering can not be neglected. Therefore, it is not surprising that the samples sintered with Pt electrodes are denser than the others, as a result of the higher sintering temperature.

The specimens treated using silver electrodes are characterized by lower density and shrinkage and larger open porosity. In this case the samples were always sintered at temperature lower than 950°C and, therefore, the densification is mainly due to FS. The

sample treated under low voltage (500 V/cm) is less dense than the others, although it was treated with the same current density and flash sintered at higher temperature. The reasons for the different densification behaviour can be related to the combination of power dissipation and furnace temperature or to the activation of different conduction mechanisms. However, this second hypothesis is actually not supported by experimental evidences (the activation energy being similar for all the considered systems).

3.2 Power dissipation during Flash Sintering

Figure 7 shows the average specific power dissipation during FS when Pt electrodes are used. The reported values take in account the sample size evolution upon sintering using the hypothesis of isotropic shrinkage. One can immediately observe that, in the tested condition, power dissipation is substantially proportional to the electrical current, J . This means that the system is not ohmic upon FS, i.e. it does not follow the second order relation:

$$P = \rho_{(T)} J^2 \quad (5)$$

where P is the specific power dissipation, $\rho_{(T)}$ the resistivity and J the current density.

Therefore, it can be assumed that the resistivity decreases with J . This should not be surprising since the system is working at higher temperature by imposing higher J .

The effect of the applied electrical field on power dissipation is less evident. Nevertheless, one can observe a slight increase of power dissipation at higher E . This is probably connected to the different FS temperature: in fact, by increasing the field, the specimen is flash sintered at lower temperature, thus decreasing the sample temperature and conductivity. The result is an increasing electrical power.

The different electrodes materials are not affecting significantly power dissipation (Fig. 8). This is probably the result of two different aspects. First, the samples sintered at low temperature (Ag) should be colder and more resistive; then, such specimens shrink less leading to lower specific power densities. Probably these two phenomena are balancing each other.

The resistivity data collected using platinum electrodes were modelled using the exponential equation:

$$\rho = \rho_0 \exp\left(\frac{Q}{RT_s}\right) \quad (6)$$

where ρ_0 is a pre-exponential constant, Q the activation energy for the conduction mechanism and T_s the sample temperature. T_s can be estimated, under the approximation that heat is completely transmitted by radiation, as:

$$T_s = \left(T_f^4 + \frac{PV}{\sigma \epsilon S}\right)^{1/4} \quad (7)$$

where T_f is the furnace temperature, V and S the specimen volume and surface, respectively, σ the Stefan-Boltzmann constant and ϵ the emissivity.

Only the data collected 1 min after the beginning of flash sintering were interpolated: this is done for being sure that the specimens were at a reasonably constant temperature and for avoiding errors due to sample evolution upon sintering. The best fit of the data was found using an emissivity of 0.65 and an activation energy of 0.94 eV. These results are still not compatible with electronic conduction. The estimated value for ρ_0 during FS was 0.0316 Ω m, much higher than that calculated from the slope of the power dissipation curve (0.0092 Ω m). The comparison between the experimental and fitting results is shown in Fig. 9. One can observe that the model provides a satisfactory approximation of all measured parameters. Even changing the emissivity in a wide range (0.9-0.2), the activation energy

varies between 0.87 and 0.95 eV. These values are slightly lower if compared to those previously measured in the experiments carried out using platinum electrodes (1.2-1.5 eV). However, one should also consider that the samples during FS achieve different final densification and this is affecting the resistivity measurement. In other words, being the specimens treated with 2 mA/mm² less dense than the others, the real current density is much higher than the “geometrical” one (calculated as the ratio between the current and the cross-section) and, therefore, the real resistivity of the material is lower than that previously estimated. It is possible to plot the real resistivity of the material (Figure 9) if some hypotheses are accepted:

- i. The main part of densification happens in the first minute after FS;
- ii. The specimen density can be approximated with the final density determined by the Archimede’s measurements;
- iii. The porosity is isotropic and homogeneously distributed.

The interpolation of the material resistivity data during FS was repeated by using the real resistivity values: an activation energy for conduction equal to 0.76 eV and an emissivity of 0.6 were estimated. Also in this case, if the emissivity is varied between 0.2 and 0.9, the activation energy does not change significantly (0.71-0.77 eV). One can point out that the activation energy measured before FS using the power dissipation plot (1.2 eV) or the onset temperature for FS (1.5 eV) should not be affected by the presence of pores within the specimens, being the density of the green bodies always the same. Therefore, the activation energy for electrical conduction undoubtedly decreases during FS. This conclusion is not straightforward; in fact, one must consider that upon FS the specimen temperature increases and this should yield to the activation of conduction mechanisms with higher

energy barrier (if different conduction mechanism are activated). Different reasons can be advanced for the observed discrepancy. Among them, the local physical/structural transformation at the grain boundary due to current concentration can be very likely considered the fundamental one, being the grain boundary a preferential diffusion path [37], as pointed out in previous works. The hypothesized rearrangement of the grain boundary can also provide an explanation for the rapid densification during FS as other authors have also already proposed [1,14]. In addition, one can suggest that the lower densification observed when Ag electrodes are used can be accounted for by the lower specimen temperature, which does not strongly affects the grain boundary structure.

4 Conclusions

Uniaxially pressed samples made by pure alumina powder can be flash sintered under electric fields in excess to 500 V/cm. Sintering temperature significantly decreases with E-field below 900°C at 1500 V/cm. The current density is shown to be the main parameter controlling the sintering rate during flash sintering and the final density of the sintered bodies.

The conduction mechanism is complex and probably several phenomena are activated, although the evidences indicate a fundamental ionic contribution to conduction.

The model describing the thermal runaway for flash sintering provides a good approximation of the correlation between the E-field and the onset temperature and indicates an activation energy for conduction coherent with the other measurements.

The electrodes material has a crucial effect on flash sintering, silver being very effective in reducing the sintering temperature in comparison to carbon or platinum.

The activation energy for conduction changes during the flash sintering phenomenon and this suggests local variations in the material structure, mainly associated to modifications or structural rearrangements at the grain boundary.

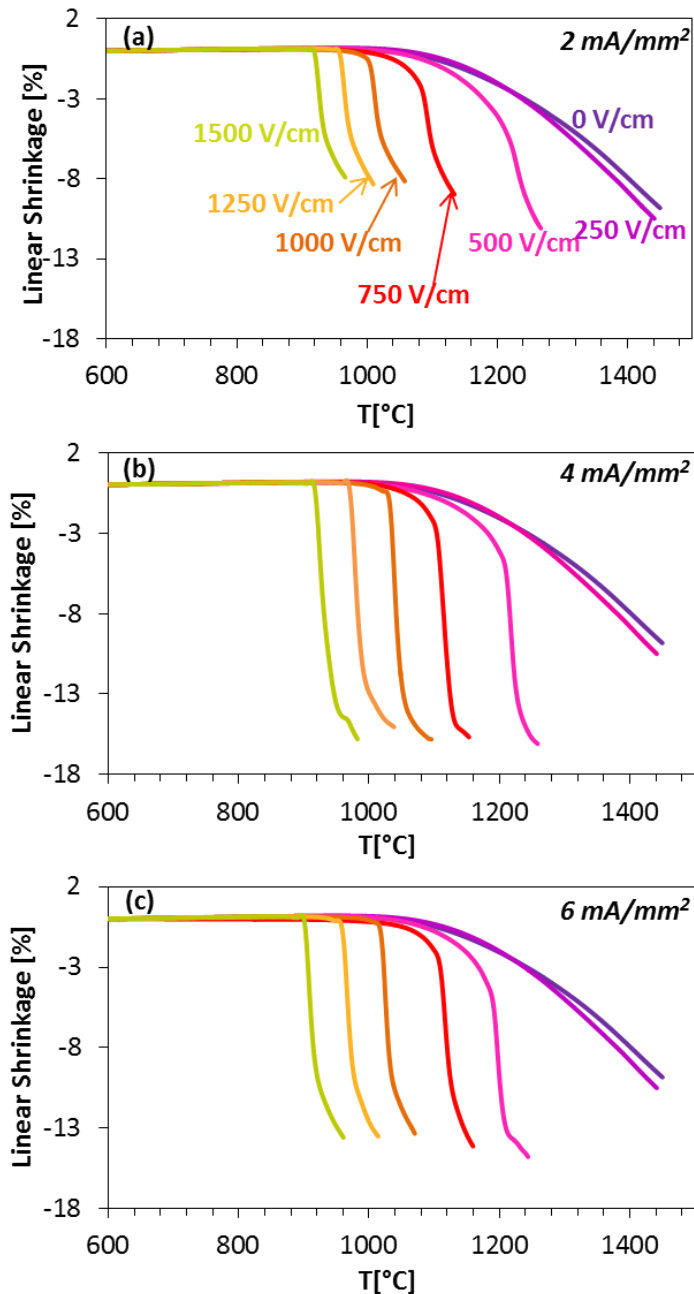


Figure 1: Shrinkage curve for alumina sintered using Pt electrodes at various voltages and with nominal current densities of 2 mA/mm² (a), 4 mA/mm² (b) and 6 mA/mm² (c).

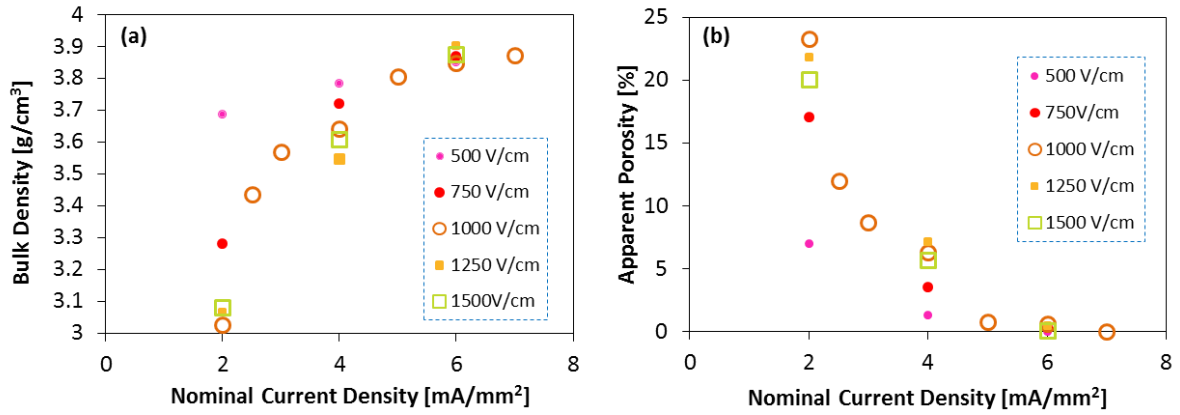


Figure 2: Bulk density (a) and apparent porosity (b) of alumina sintered between Pt electrodes as a function of the nominal current density.

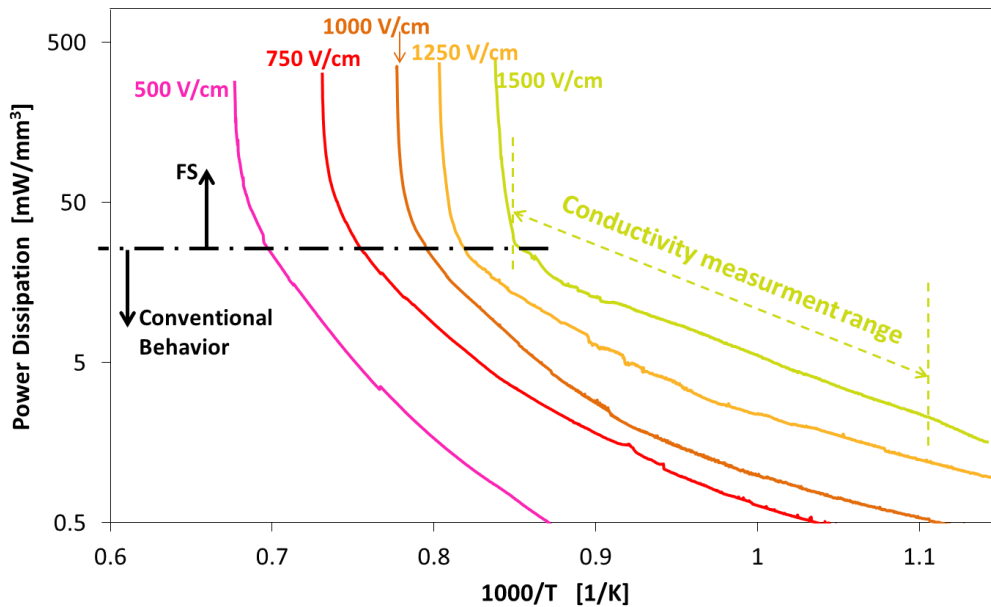


Figure 3: Specific power dissipation during FS experiments (current limit = 6 mA/mm²). The dashed line indicates the temperature range used for activation energy measurement in the sample treated under 1500 V/cm.

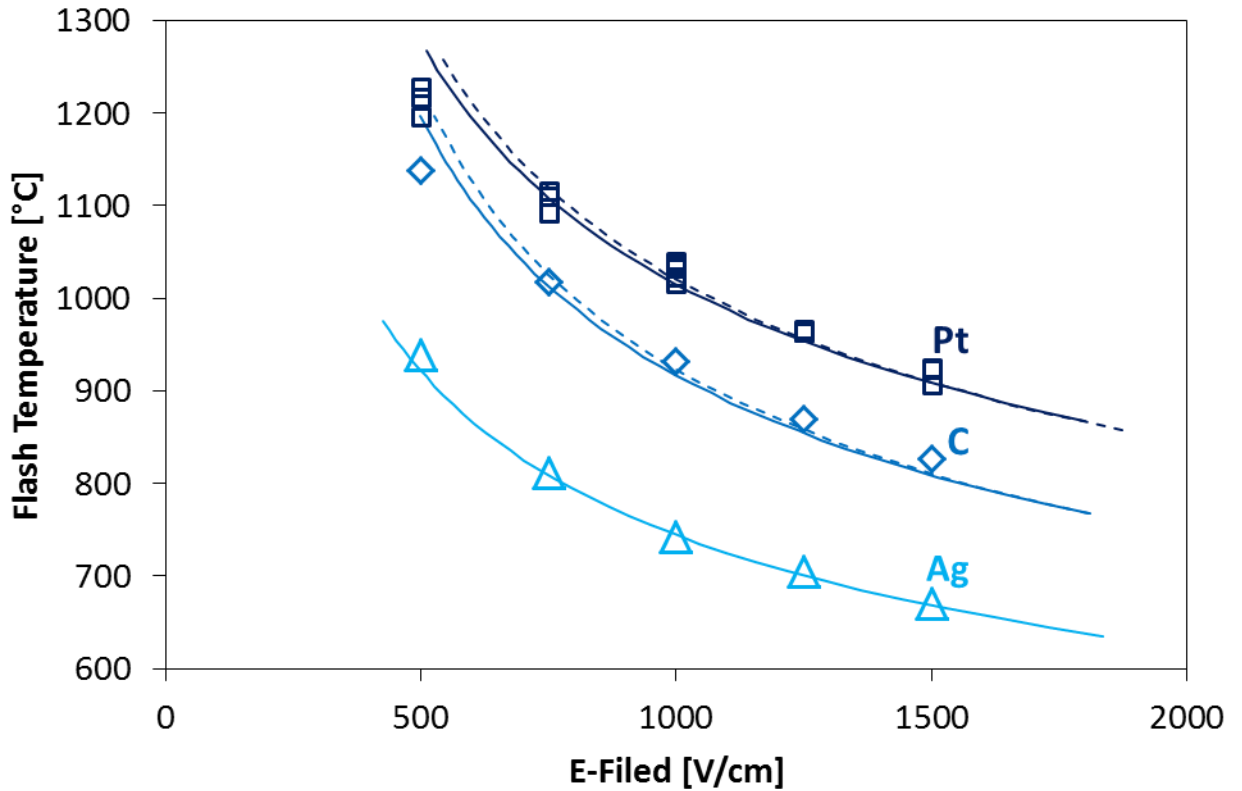


Figure 4: Onset temperature for FS as a function of the applied E-Field. The continuous curves represent the interpolating function; the dashed lines are the interpolating curves calculated removing the point at 500 V/cm.

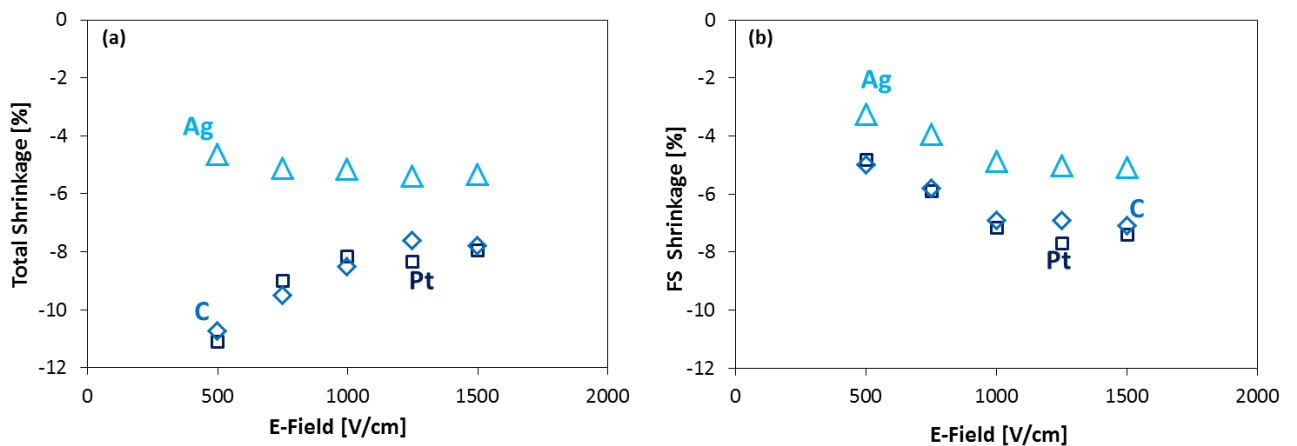


Figure 5: Total linear shrinkage upon sintering (a) and shrinkage obtained during the Flash Sintering event (b) for different electrode materials (current limit = $2\text{mA}/\text{mm}^2$).

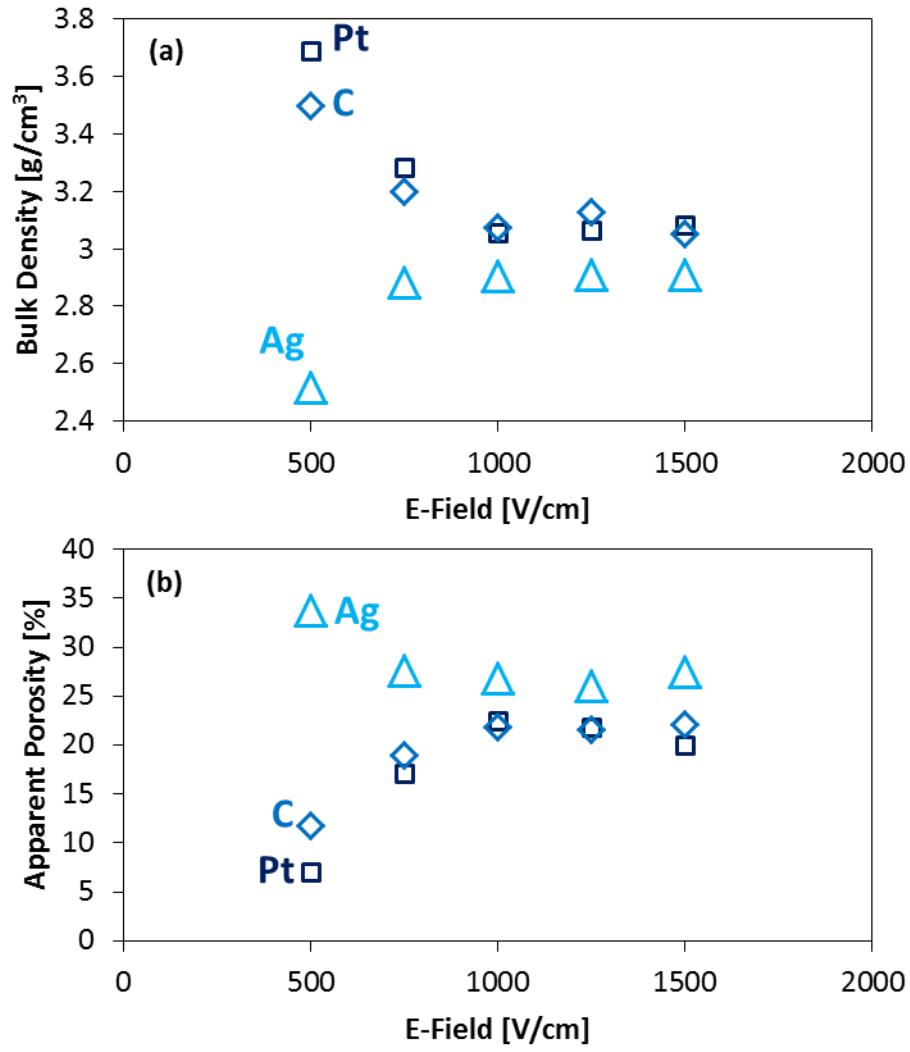


Figure 6: Bulk density (a) and apparent porosity (b) of samples flash sintered using different electrode materials at various voltages (2mA/mm²).

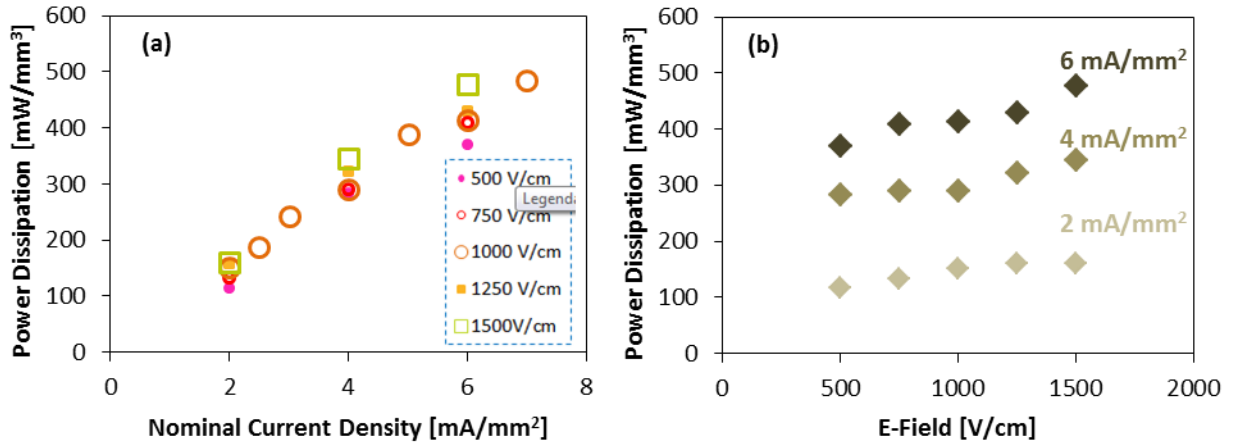


Figure 7: Average specific power dissipation during FS as a function of current density (a) and applied E-Field (b) using platinum electrodes.

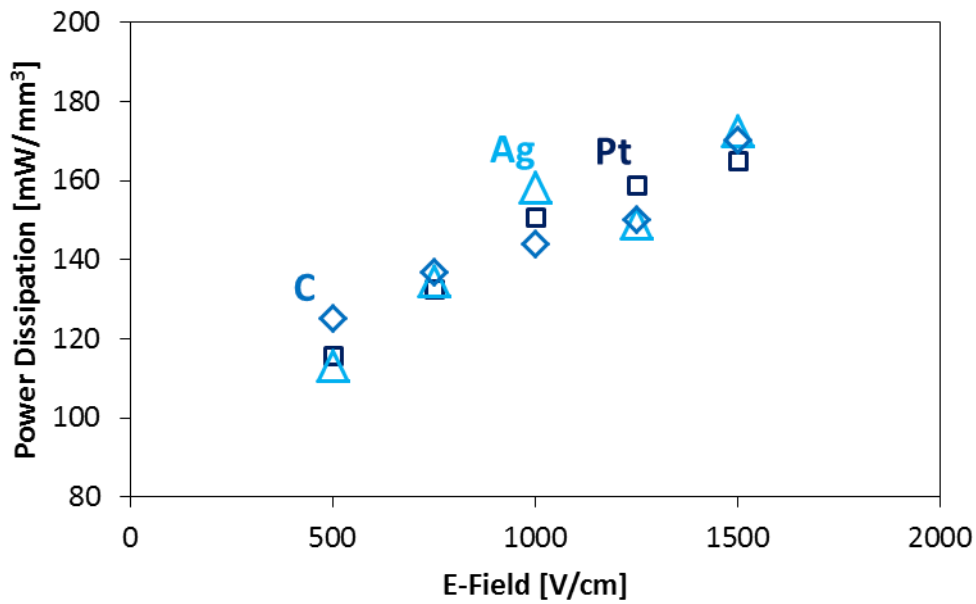


Figure 8: Average specific power dissipation during FS as a function of the applied E-Field for different electrode materials (2 mA/mm²).

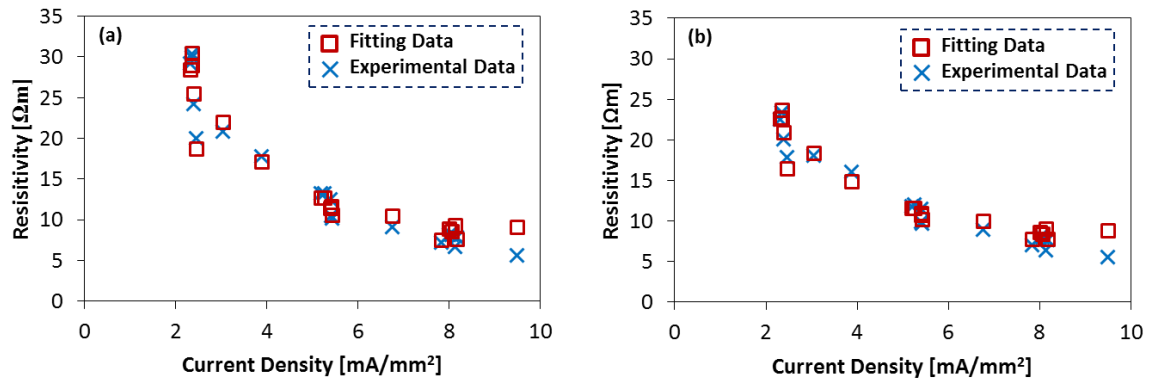


Figure 9: Resistivity during FS calculated using the geometrical parameters of the specimens (a) and real resistivity estimated taking account of the porosity (b) as a function of the measured current density. The fitting data are calculated using $Q=0.94$ eV, $\varepsilon=0.65$ (a) and $Q=0.76$ eV, $\varepsilon=0.60$ (b) and provide good approximation to the experimental results.